Optimal Restoration of Distribution Systems Considering Temporary Closed-Loop Operation

Renzo Vargas, *Member, IEEE*, Leonardo H. Macedo, *Member, IEEE*, Juan M. Home-Ortiz, and Rubén Romero, *Senior Member, IEEE*

***Abstract*—This paper presents a new mathematical model to solve the restoration problem in balanced distribution systems with distributed generators (DGs) considering closed-loop topology operation during the restorative state. The restorative state is comprised of the interval of time since the permanent fault has been isolated until the time at which the faulted zone is repaired. During this interval of time, switching operations are performed to minimize the negative effects resulting from the occurrence of a permanent fault in the network. In this way, the two main objective functions of the restoration problem are (i) to minimize the amount of load curtailment in the restored system and (ii) to minimize the number of switching operations. Conventionally, the network topology is maintained radial throughout the restorative state. In this work, the possibility of forming loops is considered for improving both objective functions. As such, a new mixed-integer second-order cone programming model is proposed, considering the temporary formation of operational loops in the restorative state, and both connected and islanded operation of the DGs. Several tests are carried out using a 53-node test system and a 2313-node system for single and multiple fault scenarios. The results obtained with the proposed model outperform the solutions achieved when only open-loop configurations are considered for the restoration problem. Moreover, it is verified that the islanded operation of the DGs provides more flexibility to the network, allowing more load to be restored.**

***Index Terms*—Closed-loop topology operation, distributed generation, distribution systems optimization, mixed-integer second-order cone programming, restoration problem.**

NOMENCLATURE

Indices:

i	Index for nodes
ij, ji	Indices for branches
s	Index for substation nodes

Sets:

Γ_N^D	Set of demand nodes
$\Gamma_{\mathbb{S}}^F$	Set of sections under fault
Γ_L	Set of real lines
Γ_L^O, Γ_L^C	Set of lines with the switch open/closed in the initial state of the system
Γ_H	Set of artificial lines connecting the artificial substation with one node at each section of the system
Γ_U	Set with real and artificial lines ($\Gamma_U = \Gamma_L \cup \Gamma_H$)
Γ_N^R	Set of nodes excluding the artificial substation node
Γ_N^S	Set of real substation nodes
Γ_N	Set of nodes including the demand nodes, real substation nodes, and the artificial substation node
Γ_N^{DG}	Set of nodes with distributed generators

Parameters:

σ_i	Load curtailment cost
τ_{ij}	Cost for closing the normally open switch at line ij
η_{ij}	Cost for opening the normally closed switch at line ij
λ_i^P, λ_i^Q	Cost of changing the active/reactive output of the distributed generator at node i
γ	Cost of loop formation
$\mathbb{S}_i$	Section that contains node i
P_i^D, Q_i^D	Active/reactive power demand at node i
$P_i^{DG_o}$,$Q_i^{DG_o}$	Prefault active/reactive generations of the distributed generator at node i
R_{ij}, X_{ij}, Z_{ij}	Resistance/reactance/magnitude of the impedance of line ij
$\hat{v}_i$	Estimate of the voltage magnitude at node i
$\underline{V}$, $\overline{V}$	Minimum/maximum voltage magnitude limit
Θ	Big-M parameter used in the disjunctive formulation for the voltage angle calculation
$\overline{I}_{ij}$	Current capacity of line ij
$\overline{S}_i^S$, $\overline{S}_i^{DG}$	Apparent power capacity of the real substation/distributed generator at node i
$\underline{\psi}_i$, $\overline{\psi}_i$	Limit for capacitive/inductive power factors of the distributed generator at node i
χ_i^{DG}	Binary parameter that indicates whether the DG at node i must only operate when connected to the main grid, if $\chi_i^{DG} = 1$, or islanded operation is allowed, if $\chi_i^{DG} = 0$.
N^{loop}	Number of basic loops allowed to be formed in the system

Continuous variables:

P_i^S, Q_i^S	Active/reactive power generation of the real substation at node i
P_{ij}, Q_{ij}	Active/reactive power flow on line ij
P_i^{DG}, Q_i^{DG}	Active/reactive power generations of the distributed generator at node i
$\hat{P}_i^{DG}$, $\hat{Q}_i^{DG}$	Active/reactive power variations of the distributed generator at node i
I_{ij}^{sqr}	Square of the current magnitude on line ij
V_i^{sqr}	Square of the voltage magnitude at node i
θ_i	Voltage phase angle at node i
ζ_{ij}, ξ_{ij}	Slack variable used in the voltage magnitude drop/voltage angle difference calculation, according to the state of the line ij
f_{ij}^e	Artificial flow on line ij used to ensure the connectivity of the network

This work was supported by the Coordination for the Improvement of Higher Education Personnel (CAPES) – Finance Code 001, the Brazilian National Council for Scientific and Technological Development (CNPq), grant 305852/2017-5, the São Paulo Research Foundation (FAPESP), under grants 2015/21972-6, 2018/20355-1, 2019/01841-5, 2019/19632-3, and 2019/23755-3, and by ENEL under the grant: PEE-00390-1062/2017 - P&D-00390-1083-2020_UFABC, ANEEL 001-2016.

R. Vargas is with the Department of Electrical Engineering, São Paulo State University, Ilha Solteira, SP, 15385-000, Brazil and the Engineering, Modeling and Applied Social Sciences Center, Federal University of ABC–UFABC, Santo André, SP, 09210-580, Brazil (e-mail: renzo.vargas@unesp.br).

L. H. Macedo, J. M. Home-Ortiz, and R. Romero are with the Department of Electrical Engineering, São Paulo State University, Ilha Solteira, SP, 15385-000, Brazil (e-mail: leohfmp@ieee.org; juan.home@unesp.br; ruben.romero@unesp.br).

g_i^c Artificial generation of the artificial substation at node i used to ensure the connectivity of the network

f_{ij}^f Artificial flow on line ij used to isolate the de-energized sections from the network

g_i^f Artificial generation of the artificial substation at node i used to isolate the de-energized sections from the network

$f_{ij,s}^c$ Artificial flow on line ij that was generated at the real substation at node s used to avoid the interconnection of substations

$g_{i,s}^c$ Artificial generation of the real substation s at node i used to avoid the interconnection of substations

Binary variables:

y_i Binary variable that indicates whether the demand at node i is supplied, if $y_i = 0$, or not, if $y_i = 1$

w_{ij} Binary variable that indicates if the switch of line ij is closed, $w_{ij} = 1$, or open, $w_{ij} = 0$

$w_{ij,s}^c$ Binary variable that indicates that the artificial flow on branch ij is from the real substation s, if $w_{ij,s}^c = 1$, or not, if $w_{ij,s}^c = 0$

$y_{i,s}^c$ Binary variable that indicates that the real substation s is supplying the demand of node i, if $y_{i,s}^c = 1$, or not, if $y_{i,s}^c = 0$

I. Introduction

THE main objective of the restoration problem is to minimize the negative effects that result from permanent faults in electric distribution networks [1]. In this way, power distribution companies are in constant search for new economic and operational alternatives to improve the system's response in order to reduce permanent fault consequences. These new alternatives must improve demand satisfaction, reconnect more users in the least possible time, avoid economical penalizations, reduce the loss of profits resulting from load disconnection, and, ultimately, improve the distribution company's reputation [2].

The presence of distributed generators (DGs) has added versatility to the operation of distribution systems in both normal operation and contingency scenarios. In normal operation, DGs can perform a dynamic regulation of the voltage profile and reduce congestion during peak load times [3]. On the other hand, during fault events, the power injection of DGs can alleviate the power flows on some lines of the network, allowing for more customers to be reconnected to the primary system [4]. Moreover, DGs with black start capability can supply energy to a group of local consumers, allowing for more loads to be reenergized [5], [6].

Distribution systems are planned with weakly meshed topologies and, usually, operated in radial configurations [7]. A radial, or open-loop, configuration facilitates the coordination and protection of a distribution system, as well as reduces the short-circuit current values in the network. On the other hand, the weakly meshed planned topology allows system reconfiguration through switching operations. The possibility of reconfiguring the network brings benefits to the distribution system, including the execution of planned maintenance procedures [8], a potential reduction of technical losses [9], and the implementation of emergency restorative actions [10].

In the literature, the closed-loop topology operation has been considered to be a temporary arrangement for load transfer [11] and an alternative to the radial operation in normal state [9]. Although the majority of distribution systems operate with a radial configuration in normal state, the closed-loop topology operation presents interesting characteristics from the system operation point of view. For instance, a network operating in a weakly meshed topology presents lower costs associated with electrical losses [9]. Moreover, system reliability could be improved when a closed-loop topology is considered for normal operation [12].

The formation of temporary loops for load transfer periods avoids in-service customers to experience short-period interruptions and long-duration voltage dips [11]. On the other hand, permanent normally closed-loop topologies are adopted so connected costumers will not experience loss of energy supply in a single fault scenario [12]. In the present work, it is considered that the network normally operates with a radial topology, while a temporary closed-loop configuration is allowed as a new strategy to improve the system's response to fault events during the restorative state.

After a permanent fault occurs in a distribution system, the faulted area must be identified and isolated through switching operations. Consequently, not only faulted regions are disconnected, but also the sections downstream to the isolated area. The service restoration problem aims to reconnect those sections by reallocating them to adjacent feeders. This reallocation of loads is executed by opening and closing sectionalizing and tie switches, respectively.

The restoration problem has been widely addressed in the literature. Heuristic methods can provide good-quality solutions with low computational times. Reference [13] presents a heuristic approach that initially closes all the switches in the network, then isolates the fault, and later, based on power flow solutions, iteratively opens switches until a feasible radial topology is obtained. Reference [14] proposes a heuristic and a relaxed mixed-integer linear programming (MILP) method for finding an approximated solution for the restoration problem. In [15], a graph-based strategy that uses Prim's algorithm for finding the minimum spanning tree is proposed to solve the restoration problem, taking into account switching costs for manual and automatic equipment. Reference [16] proposes a heuristic for the restoration problem considering network reconfiguration, while reference [17] proposes a dynamic programming algorithm for the problem. Multiagent systems have also been presented in [18] and [19] for the restoration problem in radial distribution systems.

Metaheuristic algorithms are capable of providing high-quality solutions for optimization problems with moderate computational efforts. This type of approach has been employed in [20], which presents a nondominated sorting genetic algorithm II for the restoration of distribution systems, treated as a multiobjective optimization problem. Emphasis is given to the restored load, but the number of switching operations and the type of switches involved in the process (automatic or manual) are also taken into account. Also, [21] proposes evolutionary algorithms for the restoration problem, considering single and multiple faults in the system. The authors of [22] present a three-stage approach that uses a particle swarm optimization algorithm for the restoration of distribution systems. The authors of [23] present a multiobjective evolutionary algorithm in tables with prioritization of switches and customers for obtaining the switching sequence for service restoration in distribution systems. Reference [10] presents a tabu-search-based algorithm for the restoration of distributions systems considering radial operation during the restorative state.

More recently, mathematical models have been presented for the restoration problem of radial distribution systems. References [24] and [25] present mixed-integer second-order cone programming (MISOCP) models for the restoration problem of radial distribution networks ensuring the separation of the system into radial energized and de-energized portions. Finally, other approaches based on MILP are presented in [26] and [27] for the restoration of distribution systems after severe fault events through the formation of radial microgrids, considering the islanded operation of DGs.

After analyzing the relevant literature, it is possible to conclude that the conventional solution of the restoration problem is a radial topology with the maximum amount of load reconnected and the lower number of switching operations. Although most of the distribution systems operate in radial configurations, the formation of temporary closed-loop arrangements in the restorative state is an operational proposal to improve the quality of the solutions of the restoration problem. It is important to note that this improvement is achieved without the installation of new equipment, such as voltage control devices and distributed generators, in the network. Therefore, there is no need for an economic investment to be made by distribution companies.

The main contributions of this work are:

1. A new MISOCP model for solving the distribution systems restoration problem, considering the possibility of creating temporary loops in the network during the restorative state, what gives flexibility to the restoration process, while controlling the number of loops formed. Results show that closed-loop configurations can restore more load than conventional radial topologies, both in single and multiple fault scenarios;
2. A general formulation that allows both connected and islanded operation of the DGs within the closed-loop restoration scheme;
3. Moreover, since the short-circuit current values can increase as loops are formed between feeders corresponding to different substations, as analyzed in [12], the present work also proposes a new set of constraints that avoids the interconnection of substations during the restorative state.

The solutions provided by the proposed model can be used as a guide for the dimensioning of the network's protection scheme: the distribution company can install/upgrade and coordinate the protective devices so that the most effective loops for restoration can be formed without compromising the isolation levels of equipment. This type of study, however, is outside the scope of this work.

The remainder of this paper is structured as follows: Section II presents the proposed formulation for the problem with constraints that avoid the interconnection of substations; Section III presents the results for several fault scenarios for two systems, considering or not the possibility of interconnecting substations; and Section IV presents the conclusions of the work.

II. Mathematical model

In this section, the mathematical model for the optimal restoration of distribution systems, considering closed-loop topology operation in the restorative state, is presented. The proposed formulation is an MISOCP model and considers an artificial network formed by an artificial substation connected to each section of the system through artificial lines. The artificial network is used to separate the nonrestored nodes from the main system and to control the number of basic loops formed (the definition of a basic loop is presented in [28]).

A. Objective function

The objective function, shown in (1), minimizes the nonrestored demand and penalizes: (i) changes on the operational state of the switches, (ii) changes on the dispatch of the DGs, and (iii) the number of basic loops formed.

$$\text{minimize}\, \psi = \sum_{i \in \Gamma_N^D | \mathbb{S}_i \notin \Gamma_\mathbb{S}^F} \sigma_i P_i^D y_i + \sum_{ij \in \Gamma_L^O} \tau_{ij} w_{ij} + \sum_{ij \in \Gamma_L^C} \eta_{ij}(1-w_{ij}) + \sum_{i \in \Gamma_N^{DG}} \left(\lambda_i^P \hat{P}_i^{DG} + \lambda_i^Q \hat{Q}_i^{DG} \right) + \gamma \left(\sum_{ij \in \Gamma_U} w_{ij} - |\Gamma_N^D| \right) \quad (1)$$

The first sum of the objective function ψ, shown in (1), quantifies the total nonrestored load without considering the demand at the faulted node. Therefore, if $y_i = 1$, then the node i is not restored and the objective function is penalized with a cost parameter σ_i. The second and third sums penalize the operation of the normally open and normally closed switches, respectively. The fourth term penalizes the redispatch of DGs, with $\hat{P}_i^{DG}$ and $\hat{Q}_i^{DG}$ defined in (17) and (18) as the absolute values of the differences in the active and reactive power dispatches of the DGs at node i before and after the fault. The fifth term penalizes the formation of loops, *i.e.*, the model guarantees the formation of the minimum number of basic operational loops needed to improve the value of the objective function, therefore, the cost parameter γ should be small. Note that the maximum number of basic loops that can be formed in the network is limited in (22).

B. Network operation model

The operation of the distribution system is determined by the power flow equations (2)–(8), based on the formulation presented in [24].

$$P_i^S + P_i^{DG} + \sum_{ji \in \Gamma_L} P_{ji} - \sum_{ij \in \Gamma_L} \left(P_{ij} + R_{ij} I_{ij}^{sqr} \right) = P_i^D (1 - y_i) \quad (2)$$

$$Q_i^S + Q_i^{DG} + \sum_{ji \in \Gamma_L} Q_{ji} - \sum_{ij \in \Gamma_L} \left(Q_{ij} + X_{ij} I_{ij}^{sqr} \right) = Q_i^D (1 - y_i) \quad (3)$$

$$\forall i \in \Gamma_N^R$$

$$V_i^{sqr} - V_j^{sqr} + \zeta_{ij} = 2(R_{ij} P_{ij} + X_{ij} Q_{ij}) + Z_{ij}^2 I_{ij}^{sqr} \quad \forall ij \in \Gamma_L \quad (4)$$

$$\hat{v}_i \hat{v}_j (\theta_i - \theta_j + \xi_{ij}) = X_{ij} P_{ij} - R_{ij} Q_{ij} \quad \forall ij \in \Gamma_L \quad (5)$$

$$V_j^{sqr} I_{ij}^{sqr} \geq P_{ij}^2 + Q_{ij}^2 \quad \forall ij \in \Gamma_L \quad (6)$$

$$|\zeta_{ij}| \leq \left(\overline{V}^2 - \underline{V}^2 \right) (1 - w_{ij}) \quad \forall ij \in \Gamma_L \quad (7)$$

$$|\xi_{ij}| \leq \Theta (1 - w_{ij}) \quad \forall ij \in \Gamma_L \quad (8)$$

In (2)–(4), the nonnegative variables V_i^{sqr} and I_{ij}^{sqr} are used to replace V_i^2 and I_{ij}^2, respectively, so that the resulting constraints become linear. Constraint (6) is a second-order cone constraint [29], [30].

Constraints (2) and (3) represent the active and reactive power balances in the nodes (Kirchhoff's current law) while Kirchhoff's voltage law is imposed on the system by (4)–(6). In

(4) and (5), the slack variables ζ_{ij} and ξ_{ij} are used to ignore the voltage drop and angle difference calculations in line ij when the operational state of the switch is open; thus, the variables ζ_{ij} and ξ_{ij} are limited according to (7) and (8), respectively. Otherwise, if the switch is closed, then ζ_{ij} and ξ_{ij} are equal to zero. At the substations, V_i^{sqr} is fixed at the nominal voltage, and θ_i is fixed at zero. For the nodes not affected by the fault, y_i is fixed at zero, *i.e.*, these nodes cannot be disconnected from the system during the restoration process.

Constraint (5) calculates the voltage phase angle difference $\theta_i - \theta_j$ in line ij, where $\hat{v}_i$ and $\hat{v}_j$ are the estimated voltages obtained through solving the power flow for the system when the faulted node is isolated. Note that constraint (5) is necessary only when the restoration scheme with loops is considered. Initially, $\hat{v}_i$ can be estimated as $\hat{v}_i = (\overline{V} + \underline{V})/2$.

C. Physical and operational limits

The physical and operational limits of the distribution system are presented in (9)–(13).

$$\underline{V}^2 \leq V_i^{sqr} \leq \overline{V}^2 \qquad \forall i \in \Gamma_N^D \tag{9}$$

$$0 \leq I_{ij}^{sqr} \leq \overline{I}_{ij}^2 w_{ij} \qquad \forall ij \in \Gamma_L \tag{10}$$

$$|P_{ij}| \leq \overline{VI}_{ij} w_{ij} \qquad \forall ij \in \Gamma_L \tag{11}$$

$$|Q_{ij}| \leq \overline{VI}_{ij} w_{ij} \qquad \forall ij \in \Gamma_L \tag{12}$$

$$(P_i^S)^2 + (Q_i^S)^2 \leq \left(\overline{S}_i^S\right)^2 \qquad \forall i \in \Gamma_N^S \tag{13}$$

Constraint (9) determines the voltage limits in the demand nodes of the system, while (10) determines the current limit in line ij according to the state of the switch of the line. In a similar way, constraints (11) and (12) limit the active and reactive power flows in line ij. The limit of power injected by a real substation is presented in (13) as a quadratic constraint. It should be noted that, for the lines without a switch, $w_{ij} = 1$.

D. Distributed generators operation model

The operation of the dispatchable DGs is represented by the set of constraints (14)–(18).

$$(P_i^{DG})^2 + (Q_i^{DG})^2 \leq \left(\overline{S}_i^{DG}\right)^2 (1 - y_i) \qquad \forall i \in \Gamma_N^{DG} \tag{14}$$

$$P_i^{DG} \geq 0 \qquad \forall i \in \Gamma_N^{DG} \tag{15}$$

$$-P_i^{DG} \tan(\cos^{-1}(\underline{\psi}_i)) \leq Q_i^{DG} \leq P_i^{DG} \tan(\cos^{-1}(\overline{\psi}_i)) \quad \forall i \in \Gamma_N^{DG} \tag{16}$$

$$|P_i^{DG_o} - P_i^{DG}| \leq \hat{P}_i^{DG} \qquad \forall i \in \Gamma_N^{DG} \tag{17}$$

$$|Q_i^{DG_o} - Q_i^{DG}| \leq \hat{Q}_i^{DG} \qquad \forall i \in \Gamma_N^{DG} \tag{18}$$

Constraint (14) is the apparent power limit for the DG at node i, and requires that a DG can operate only if it is connected to an in-service node. Constraint (15) establishes that a DG can only inject active power to the system. Constraint (16) limits the reactive power injection of the DG at node i considering its power factor limits. Constraints (17) and (18) calculate the variations in the active and reactive power dispatches of the DGs before the fault and in the restored state of the system.

Constraints (19)–(21) represent an artificial flow balance in the network to ensure the connectivity of the network avoiding the islanded operation of some DGs.

$$\sum_{ji \in \Gamma_L} f_{ji}^e - \sum_{ij \in \Gamma_L} f_{ij}^e + g_i^e = \chi_i^{DG}(1 - y_i) \qquad \forall i \in \Gamma_N^R \tag{19}$$

$$|f_{ij}^e| \leq |\Gamma_N^R| w_{ij} \qquad \forall i \in \Gamma_L \tag{20}$$

$$0 \leq g_i^e \leq |\Gamma_N^R| \qquad \forall i \in \Gamma_N^S \tag{21}$$

It should be noted that the variable g_i^e is fixed at zero at all nodes, except at the real substation nodes, and $\chi_i^{DG} = 0$ at nodes without DGs. Constraint (19) establishes an artificial flow balance in the system. Note that, if $\chi_i^{DG} = 1$, representing a DG that can only operate when connected to the main grid, and $y_i = 0$, representing a de-energized node, then a unity artificial demand is considered at node i, and this demand can only be supplied by a substation, requiring that there must exist a path between node i and a substation. On the other hand, if χ_i^{DG} =0, representing a DG that can operate islanded, or $y_i = 0$, then it is not required that the node i is connected to a substation. Constraint (20) limits the artificial flow on the branches according to their statuses. Finally, constraint (21) limits the artificial generation at the substation nodes.

E. Constraints for controlling the network topology

After the fault isolation process, several nodes lose energy supply, and switching operations are necessary to reconnect these nodes to adjacent feeders belonging to the main grid. In this regard, the proposed model creates two systems, separating the main grid and the nodes that cannot be restored in a secondary grid. The secondary grid is an artificial system fed by the artificial substation that can be directly connected with all the system's sections through artificial lines. Fig. 1 (a) presents an illustrative system with two substations (at nodes 100 and 101), ten demand nodes (nodes 1–10), and one artificial substation (at node 200), which is connected to each node through artificial branches. The dotted lines represent the lines disconnected from the system while the continuous lines are operating. Note that the initial operation of the system is radial.

The basic radiality condition in distribution systems can be guaranteed when the number of lines in operation (including the artificial lines) is equal to the number of demand nodes and the system is connected [31]. Constraint (22) is used to limit the maximum number of basic loops in the system through the parameter N^{loop}.

$$|\Gamma_N^D| \leq \sum_{ij \in \Gamma_U} w_{ij} \leq |\Gamma_N^D| + N^{loop} \tag{22}$$

In (22), if $N^{loop} = 0$, then the resulting topology is a radial system; otherwise, if $N^{loop} \geq 1$, the restoration process allows for a meshed topology for the network, in which N^{loop} is the number of basic operational loops allowed to be created in the network. The maximum value for N^{loop} is the number of normally open switches in the system before the fault.

Constraints (23)–(27) ensures that the real and the artificial networks are separated from each other and each one of them presents connected topologies.

$$\sum_{ji \in \Gamma_U} f_{ji}^f - \sum_{ij \in \Gamma_U} f_{ij}^f + g_i^f = y_i \qquad \forall i \in \Gamma_N \tag{23}$$

$$|f_{ij}^f| \leq |\Gamma_N| w_{ij} \qquad \forall ij \in \Gamma_U \tag{24}$$

$$f_{ij}^f \geq 0 \qquad \forall ij \in \Gamma_H \tag{25}$$

$$\sum_{ji \in \Gamma_U} w_{ji} + \sum_{ij \in \Gamma_U} w_{ij} \geq 1 \qquad \forall i \in \Gamma_N^D \tag{26}$$

$$|y_i - y_j| \leq 1 - w_{ij} \qquad \forall ij \in \Gamma_L \tag{27}$$

In (23)–(27), the set Γ_N is the set of nodes, including the demand nodes, real substation nodes (the substations of the system are referred to as *real substations*, as opposed to the artificial substation), and the artificial substation node. It should be

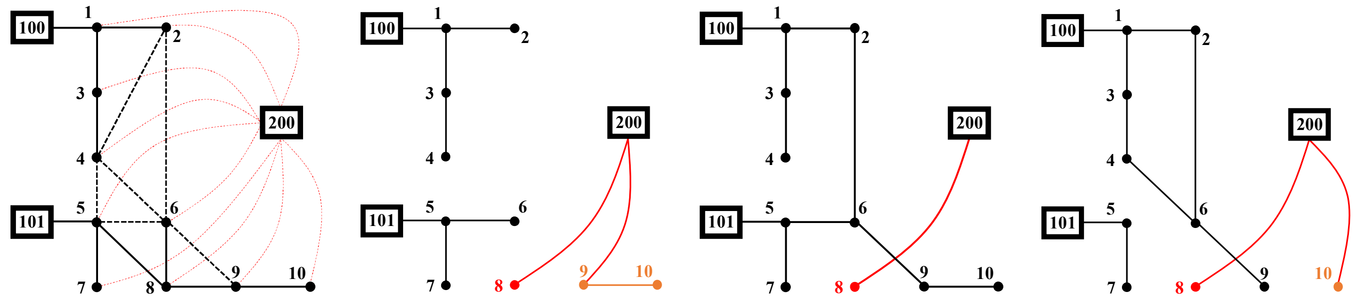

Fig. 1 Illustrative 12-node system for the network topology constraints: (a) prefault radial configuration, (b) topology considering radial restoration, (c) temporary closed-loop operation, (d) temporary closed-loop operation avoiding the interconnection of substations.

noted that the variable g_i^f is fixed at zero at all nodes, except at the artificial substation node. Also, the variable y_i is fixed at zero at all the substations, including the artificial one. For all the lines with a switch and with one terminal at the section (or sections) under fault, w_{ij} is fixed at zero to isolate the section under fault. For all the nodes in the section under fault, y_i is fixed at one. Finally, y_i is fixed at zero at all nodes not affected by a fault, i.e., these nodes cannot be de-energized in the restoration procedure.

The set of constraints (23)–(27) connects the nodes that cannot be restored to the artificial network. Equation (23) represents the artificial power flow balance on the network that only connects the nonrestored nodes. When $y_i = 1$, there must be a path connecting the artificial substation to the section that contains node i, so that the unitary artificial demand represented by y_i is supplied. Constraint (24) limits the artificial power flow on the lines of the system according to the state of operation of the switch on the real or artificial line ij. Constraint (25) imposes that the artificial power flows through the lines directly connected to the artificial substation be nonnegative, in which it is assumed that node i is the artificial substation node. Constraint (26) is a fencing constraint that ensures that all the load nodes have at least one line (real or artificial) connected to it, while in (27), if the switch of line ij is closed ($w_{ij} = 1$), then both nodes, i and j, have the same operational state ($y_i = y_j$), and these nodes are either connected to the main or to the artificial network.

To facilitate the understanding of the presented formulation, Fig. 1 (b)–(d) illustrates different restorative topologies for the 12-node system assuming a permanent fault at node 8. In this figure, branches 5-8, 6-8, and 8-9 are opened to isolate the fault, and as a result, nodes 9 and 10 are de-energized. The binary variable y_i is fixed at zero at nodes 1, 2, 3, 4, 5, and 7, not affected by the fault, therefore, these nodes must be energized in the solution of the restoration problem.

Assuming that each node has a demand, constraints (2) and (3) will require that the energized system is connected, i.e., there must be at least one path from a substation (at node 100 and 101) to each energized node, with $y_i = 0$. Also, constraints (23)–(26) will require the existence of a path from each de-energized node (with $y_i = 1$) to the artificial substation (at node 200). Moreover, constraint (27) will require that the energized and de-energized nodes are disconnected from each other.

According to [31], if $N^{loop} = 0$, and if there is a path from each node to each substation, constraint (22) ensures that the resulting topology is radial. Fig. 1 (b) shows this situation, for which $|\Gamma_N^D| = 10$, requiring that the number of branches connected to the system is also 10. The entire system will, therefore, present a radial configuration. Note that, in this case, nodes 8–10 are de-energized and connected to the artificial substation, due to the operational constraints of the network.

By letting $N^{loop} > 0$, up to N^{loop} branches can be connected, and the resulting topologies can present a closed-loop topology. Fig. 1 (c) illustrates this case for $N^{loop} = 1$, in which 11 branches are operating (ten in the real system and one in the artificial network), and one loop is formed among the substations at nodes 100 and 101. Note that, in this case, only node 8 is de-energized, and, therefore, connected to the artificial network.

Fig. 1 (d) also illustrates a case in which the resulting topology of the system presents one loop, but the loop does not interconnect the substations at nodes 100 and 101. Note that, in this case, node 10 remains de-energized, due to the operational constraints of the network. The next section will introduce additional constraints that avoid the interconnection of substations when temporary closed-loop operation is allowed.

F. Constraints that avoid the interconnection of substations

The optimization model (1)–(27) provides solutions to the restoration problem allowing loops in the network topology, including the interconnection of substations. If it is required to avoid the interconnection of substations, constraints (28)–(34) restrict the formation of operational loops only among the feeders of the same substation. These constraints consider one artificial network for each substation, with the same topology of the real network, and use the variable $y_{i,s}^c$ to indicate which substation s feeds the demand at node i, according to the statuses of the switches, given by w_{ij}.

$$\sum_{ji \in \Gamma_L} f_{ji,s}^c - \sum_{ij \in \Gamma_L} f_{ij,s}^c + g_{i,s}^c = y_{i,s}^c \qquad \forall i \in \Gamma_N^R, s \in \Gamma_N^S \tag{28}$$

$$|f_{ij,s}^c| \leq |\Gamma_N| w_{ij,s}^c \qquad \forall ij \in \Gamma_L, s \in \Gamma_N^S \tag{29}$$

$$\sum_{s \in \Gamma_N^S} w_{ij,s}^c = w_{ij} \qquad \forall ij \in \Gamma_L \tag{30}$$

$$\sum_{s \in \Gamma_N^S} y_{i,s}^c = 1 - y_i \qquad \forall i \in \Gamma_N^R \tag{31}$$

$$|y_{i,s}^c - y_{j,s}^c| \leq 1 - w_{ij} \qquad \forall ij \in \Gamma_L, s \in \Gamma_N^S | \mathbb{S}_i \neq \mathbb{S}_j \tag{32}$$

$$y_{i,s}^c = y_{j,s}^c \qquad \forall ij \in \Gamma_L, s \in \Gamma_N^S | \mathbb{S}_i = \mathbb{S}_j \tag{33}$$

$$w_{ij,s}^c = w_{kl,s}^c \qquad \forall ij, kl \in \Gamma_L, s \in \Gamma_N^S | \mathbb{S}_i = \mathbb{S}_k \wedge \mathbb{S}_j = \mathbb{S}_l \tag{34}$$

In (28)–(34), $g_{i,s}^c$ can be different from zero only for $i = s$ and at the real substation nodes.

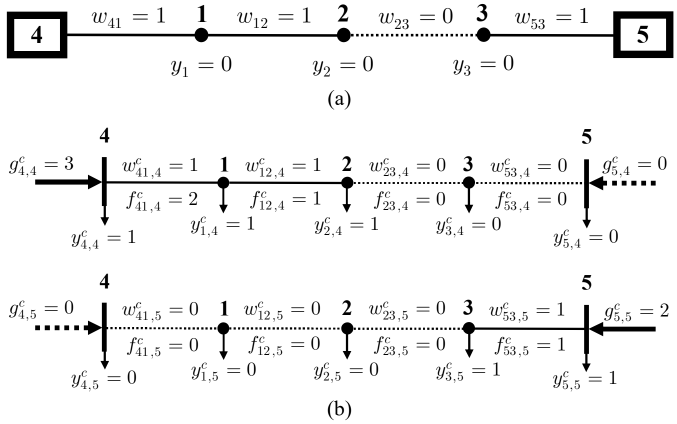

Fig. 2 (a) Illustrative 5-node network and (b) representation of the artificial networks that avoid the interconnection of substations for the 5-node network.

Constraint (28) represents the artificial flow balance on the artificial grid; this constraint is formulated for all the nodes, except the artificial substation node, and ensures that the in-service node i, with $y^c_{i,s}=1$, is connected to the corresponding substation s, from the set of real substations nodes, Γ^S_N. Constraints (29) and (30) impose that if a line ij is operating ($w_{ij}=1$), then only one $f^c_{ij,s}$ is different from zero, ensuring that the artificial flow on branch ij is from only one substation. Constraint (31) relates the binary variable y_i, which represents the connection state of a node i, with the binary variable $y^c_{i,s}$, which indicates which real substation s is supplying the demand of node i. If $y_i=0$, node i is supplied from exactly one substation s from set Γ^S_N; otherwise, if $y_i=1$, node i is disconnected from the system. Constraint (32) ensures that, if the switch of line ij is closed ($w_{ij}=1$), then both nodes i and j have the same substation s supplying their demands. If both nodes i and j belong to the same section, (33) also ensures that they will be supplied by the same substation. Constraint (34) imposes that, if two lines, ij and kl, belong to the same section, their artificial flows were originated at the same substation.

In addition, the variables $g^c_{i,s}$ and $y^c_{i,s}$ must be fixed, as shown in (35)–(38).

$$g^c_{i,s}=0 \qquad \forall i\in\{\Gamma_N-\Gamma^S_N\}, s\in\Gamma^S_N \tag{35}$$

$$g^c_{i,s}=0 \qquad \forall i\in\Gamma^S_N, s\in\Gamma^S_N | i\neq s \tag{36}$$

$$y^c_{i,s}=0 \qquad \forall i\in\Gamma^S_N, s\in\Gamma^S_N | i\neq s \tag{37}$$

$$y^c_{i,s}=1 \qquad \forall i\in\Gamma^S_N, s\in\Gamma^S_N | i= s \tag{38}$$

Constraint (35) fixes the artificial generation, $g^c_{i,s}$, at zero at all load nodes, and (36) fixes $g^c_{i,s}$, $i\neq s$, at zero at all real substation nodes, while (37) and (38) fix $y^c_{i,s}$ for all real substation nodes. The optimization model (1)–(34) is an MISOCP model that guarantees convergence to the optimal solution via commercial optimization solvers.

Fig. 2 presents the values for the binary and continuous variables involved in the set of constraints (28)–(38). In this example, the network is composed of two substations, at nodes 4 and 5. These substations feed the load nodes 1, 2, and 3. The set of closed lines is {4-1, 1-2, 5-3}, thus the values for variable w_{ij} over this set is equal to 1 ($w_{41}=w_{12}=w_{53}=1$), while line 2-3 is opened, and therefore $w_{23}=0$. In this case, the demand of all the load nodes are supplied, thus the values for y_i is equal to 0 in all the load nodes, as presented in Fig. 2 (a). Note that (28)–(38) is applied only in the real network. Two artificial networks are presented in Fig. 2 (b), one for each real substation. They are used to determine which substation is feeding each load node and to avoid the interconnection of substations.

In constraint (30), the operational state of the real lines determines the state of the artificial lines, thus, in this case, the open branch 2-3 ($w_{23}=0$) obligates the corresponding artificial lines to be open ($w^c_{23,4}=w^c_{23,5}=0$); on the other hand, the closed line 4-1 ($w_{41}=1$), obligates only one artificial line, $w^c_{41,4}$ or $w^c_{41,5}$, to be closed. This situation is the same for lines 1-2 and 5-3.

In constraint (31), the operational state of the load nodes determines the state of the artificial loads. For node 1, this constraint obligates one artificial load, $y^c_{1,4}$ or $y^c_{1,5}$, to be equal to 1. The same is valid for nodes 2 and 3.

Each artificial network is related to one real substation. Besides that, in each of these networks, only one substation can supply the artificial demands. Constraint (35) fixes in zero all the injections from other substations. In this case, for the first artificial network (corresponding to the substation node 4), the artificial generation $g^c_{5,4}$ (corresponding to the substation node 5) is fixed in zero. Similarly, $g^c_{4,5}$ is fixed in zero in the other network. Constraints (37) and (38) fix the artificial demands at the substation nodes.

The values for the artificial flow variables, $f^c_{ij,s}$, and the artificial injections, $g^c_{s,s}$, are determined by the flow balance constraint (28). Note that, constraint (32) requires that nodes 2 and 3 are supplied by different substations, since $w_{23}=0$. Therefore, the artificial demands at these nodes have different values, i.e., $y^c_{2,4}\neq y^c_{3,4}$ and $y^c_{2,5}\neq y^c_{3,5}$.

The only feasible solution to the set of constraints (28)–(38) has $y^c_{1,4}=1$, $y^c_{2,4}=1$, $y^c_{3,4}=0$, $y^c_{1,5}=0$, $y^c_{2,5}=0$, and $y^c_{3,5}=1$, indicating that nodes 1 and 2 are connected to the substation at node 4, while node 3 is connected to the substation at node 5.

III. Tests and Results

A 53-node test system [24] and a 2313-node system of a Colombian oil company [32] are used to demonstrate the efficiency and robustness of the proposed mathematical model. The 53-node test system has three substations and 50 load nodes, each one representing a section of the system, with total active and reactive power demands of 45,668.70 kW and 22,118.24 kVAr, respectively. The nominal voltage is 13.8 kV, with a minimum voltage limit of 0.95 p.u. and a maximum limit of 1.05 p.u. To analyze the influence of the DGs in the restoration problem, three DGs are installed at nodes 5, 15, and 47 of the 53-node system. The 2313-node system has six substations, two DGs, and 2307 load nodes with total active and reactive power demands of 59,578.65 kW and 28,855.25 kVAr, respectively. The nominal voltage is 14.4 kV, with a minimum and maximum voltage limits of 0.95 p.u. and 1.05 p.u, respectively. Complete data for both systems can be found in [32].The optimization model was implemented in AMPL [33] and solved with the commercial solver CPLEX v12.9 [34] on a computer with a 3.2 GHz Intel® Core™ i7–8700 processor and 16 GB of RAM.

A. Results for the 53-node system

Six study cases are presented in this section:

TABLE I

RESULTS FOR THE 53-NODE SYSTEM WITHOUT DGs – CASE I

Faulted node	# of loops	Switching operations	Switches opened	Switches closed	Disconnected nodes	Active load curtailment (kW)	Active load restored (%)	Time (s)
3	0	9	5-4, 28-6, 27-8, 26-27, 34-33	28-27, 8-33, 35-40, 28-50	5, 6, 26	3118.50	57.94	4.96
	2	12	7-4, 6-5, 37-43, 17-9, 34-33	10-31, 18-17, 8-25, 28-27, 8-33, 35-40, 28-50	4, 5	2564.10	65.42	5.09
	5	12	5-4, 8-7, 17-9, 26-27	10-31, 18-17, 8-25, 28-27, 8-33, 35-40, 10-38, 28-50	4, 7, 26	2286.90	69.16	3.88
14	0	5	16-40, 42-41, 47-42	35-40, 28-50	15, 16, 41, 46, 47	4851.00	40.17	2.87
	1	6	16-40, 42-41, 46-47	28-27, 35-40, 28-50	15, 16, 41, 46	4158.00	48.72	3.12
	4	12	22-9, 24-23, 16-40, 46-47	10-31, 104-22, 8-25, 28-27, 40-41, 35-40, 10-38, 28-50	15, 16, 46	3534.30	56.41	3.33
11, 14	0	12	31-37, 22-9, 44-45, 38-44, 33-39, 16-40	10-31, 13-12, 104-22, 8-33, 35-40, 10-38	15, 16, 41, 42, 44, 46, 47, 48, 49, 50	8108.10	52.82	32.11
	1	18	31-37, 22-9, 44-45, 38-44, 33-39, 36-35, 16-40, 42-41, 49-48	10-31, 13-12, 104-22, 8-25, 8-33, 40-41, 35-40, 10-38, 28-50	15, 16, 36, 42, 44, 46, 47, 48	6791.40	60.48	7.79
	2	11	31-37, 22-9, 44-45, 48-42	10-31, 13-12, 104-22, 8-25, 8-33, 10-38, 28-50	15, 16, 40, 41, 42, 46, 47	6652.80	61.29	6.83
11, 14, 21	0	11	45-12, 22-9, 32-39, 33-39, 16-40	13-12, 18-17, 104-22, 8-33, 35-40, 10-38	15, 16, 32, 41, 42, 46, 47, 48, 49, 50	8316.00	57.45	18.17
	1	17	45-12, 22-9, 32-39, 33-39, 36-35, 16-40, 42-41, 49-48	13-12, 18-17, 104-22, 8-25, 8-33, 40-41, 35-40, 10-38, 28-50	15, 16, 32, 36, 42, 46, 47, 48	6999.30	64.18	6.69
	2	16	31-37, 28-6, 44-45, 38-44, 33-39, 42-41, 47-42	10-31, 13-12, 18-17, 104-22, 8-25, 28-27, 8-33, 10-38, 28-50	15, 16, 40, 41, 44, 46, 47	6791.40	65.25	4.83

- *Case I:* the formation of loops between feeders corresponding to the same or different substations is allowed and DGs are not considered in the system (see Table I);
- *Case II:* the formation of loops is allowed only among feeders of the same substation and DGs are not considered in the system (see Table II);
- *Case III:* the formation of loops between feeders corresponding to the same or different substations is allowed and DGs are allowed to operate only when connected to the main grid (see Table III);
- *Case IV:* the formation of loops is allowed only among feeders of the same substation and DGs are allowed to operate only when connected to the main grid (see Table IV);
- *Case V:* the formation of loops between feeders corresponding to the same or different substations is allowed and the islanded operation of the DGs is allowed (see Table V);
- *Case VI:* the formation of loops is allowed only among feeders of the same substation and the islanded operation of the DGs is allowed (see Table VI).

The proposed model can restore a distribution system for both single and multiple permanent fault events. Thus, for all the study cases, single fault events at the critical nodes 3 and 14, and multiple fault events at the nodes' groups {11, 14}, and {11, 14, 21} are analyzed.

In Case I, the interconnection of substations is allowed in the solution of the original 53-node system without DGs. For this purpose, constraints (28)–(34) are not considered in the formulation. It is assumed that each line of the test system has a switch and the power supply must be maintained at the nodes that were not disconnected after the isolation of the faulted area. All switches are of the same type, and there are no priority loads. The following subsections present a discussion of the results obtained in each fault scenario. Table I summarizes the results obtained for Case I and the computational times to solve each instance of the problem.

1) Case I – Fault at node 3: In this case, a fault at node 3 was analyzed. Lines 101-3 and 4-3 are opened to isolate the faulted section, and both switching operations are not accounted in the final solution. The load at node 3 (485.10 kW and 234.93 kVAr) is not restorable. The results in Table I show that, by increasing the number of loops allowed in the system from zero to five, the active load restored increases from 57.94% to 69.16%. However, when only one loop is allowed to be formed, the solution is radial (the same one when no loop is allowed in the system). Also, when three or four loops are allowed in the system, no improvement is verified in comparison with the solution with two loops. Finally, by setting the number of loops at its maximum value, *i.e.*, the number of normally open switches in the prefault configuration, no additional improvement is achieved.

2) Case I – Fault at node 14: In this case, the results are obtained for a permanent fault at node 14. The number of loops allowed in the system is increased sequentially to identify its influence in the quality of the solution. The faulted node 14, with a load of 693.00 kW and 335.64 kVAr, is disconnected by opening the lines between nodes 102-14, 15-14, and 14-46. As a first analysis, no loop is admitted in the restoration process. According to Table I, in the obtained solution, 40.17% of the active load is restored. For the next analysis, the formation of one loop is allowed in the restoration process, and the restored load is increased to 48.72%. When two and three loops are allowed to be formed in the restoration process, the obtained solution is the same as the result previously obtained when one loop is considered. When assuming the formation of four loops, a solution with better quality is obtained: 56.41% of the active load is restored. By increasing the number of loops allowed in the restorative state above four, no additional improvement is obtained.

3) Case I – Fault at nodes 11 and 14: Permanent faults at the critical nodes 11 and 14 are considered in this case. As such, a total demand of 900.9 kW and 436.36 kVAr is not restorable. Lines 102-14, 15-14, 14-46, 12-11, and 102-11 are opened to isolate the faulted nodes. According to Table I, by allowing zero, one, and two loops in the system, the percentages of the

TABLE II
RESULTS FOR THE 53-NODE SYSTEM THAT AVOID THE INTERCONNECTION OF SUBSTATIONS WITHOUT DGS – CASE II

Faulted node	# of loops	Switching operations	Switches opened	Switches closed	Disconnected nodes	Active load curtailment (kW)	Active load restored (%)	Time (s)
3	0	9	5-4, 28-6, 27-8, 26-27, 34-33	28-27, 8-33, 35-40, 28-50	5, 6, 26	3118.50	57.94	5.19
14	1	6	16-40, 42-41, 46-47	28-27, 35-40, 28-50	15, 16, 41, 46	4158.00	48.72	3.39
11, 14	1	16	31-37, 22-9, 28-6, 44-45, 32-39, 36-35, 16-40, 50-49	10-31, 13-12, 104-22, 28-27, 8-33, 35-40, 10-38, 28-50	15, 16, 32, 36, 41, 42, 46, 47, 48, 49	7969.50	53.63	19.31
11, 14, 21	1	9	31-37, 22-9, 44-45	10-31, 13-12, 18-17, 104-22, 8-33, 10-38	15, 16, 40, 41, 42, 46, 47, 48, 49, 50	8108.10	58.51	9.18

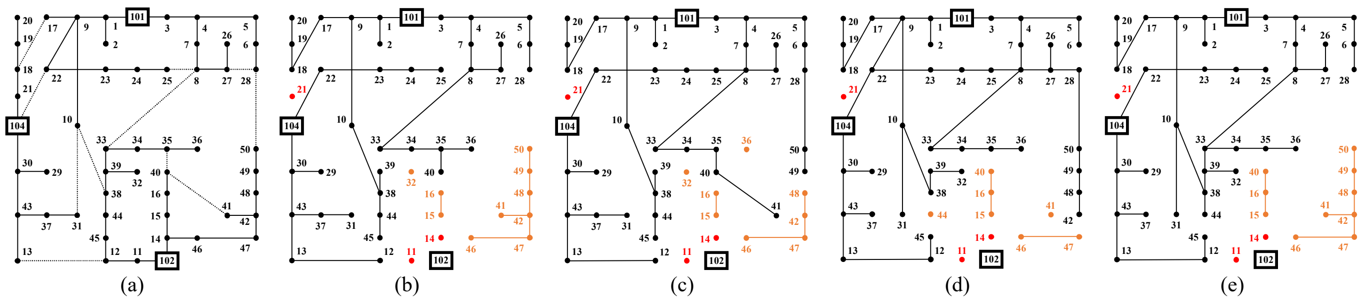

Fig. 3 (a) Prefault configuration of the 53-node system without DGs. Restoration schemes considering simultaneous faults at nodes 11, 14, and 21 with (b) a radial configuration, (c) one basic loop, (d) two basic loops, and (e) one basic loop without the interconnection of substations.

active load restored are, respectively, 52.82%, 60.48%, and 61.29%. When the number of loops allowed is set at its upper limit, the solution has the same quality as the one obtained considering two loops.

4) Case I – Fault at nodes 11, 14, and 21: A multiple fault scenario is considered in this case. Permanent faults at nodes 11, 14, and 21 are assumed in the network, totaling a nonrestorable load of 2148.30 kW and 1040.50 kVAr. The switches in lines 102-14, 15-14, 102-11, 12-11, 104-21, 21-18, and 14-46 are opened to isolate the faulted nodes. According to Table I, by allowing zero, one, and two loops in the system, the percentages of the active load restored are, respectively, 57.45%, 64.18%, and 65.25%. Finally, when the number of loops allowed in the restorative state is set to its maximum value, the optimal solution presents the same quality as the result with two loops.

5) Case I – Comments on the results considering closed-loop topology operation: Based on the results summarized in Table I, the following can be observed:

- In all the cases, for single and multiple fault scenarios, solutions of better quality are found when the formation of operational loops is allowed in the restorative state.
- For the single fault scenarios at nodes 3 and 14, the radial solutions presented in Table I are the same obtained by [24] when the nodes not affected by the fault must remain connected to the system in the solution of the restoration problem.
- The improvement in the quality of the solutions is directly associated with the number of loops allowed in the system. As can be seen in Table I, as the number of loops allowed increases, the quality of the solutions improves.
- Increasing the number of loops in only one unit does not necessarily improve the quality of the obtained result.
- The number of loops that can be formed in the restorative state is limited by constraint (22). In this restriction, the maximum number of loops, N^{loop}, is predefined and controls the number of operational loops that can be formed in the final solution. However, for each case, there is an optimal number of loops, as shown in Table I. For instance, the optimal number of loops in the case of a permanent fault at node 3 is five; meanwhile, the optimal number of loops for a fault at node 14 is four. In the proposed formulation, the optimal number of loops can be directly found by the model, by setting the number of loops at its maximum value. In other words, when the maximum value of the loops that can be formed is equal to the number of normally open switches in the prefault configuration, the model automatically finds the optimal number of loops. This fact is explained by the last term in the objective function (1). In this term, the objective function penalizes the formation of loops, guaranteeing the minimal number of loops necessary to improve the value of the objective function.
- The computational times to solve the problem are of only a few seconds in all the cases, and, by increasing the number of loops allowed to be formed in the system, the computational time is usually reduced.

Case II considers the possibility of forming temporary loops in the system for improving service restoration, but the loops are restricted to feeders corresponding to the same substation and DGs are not installed in the system. For this purpose, the complete model (1)–(34) is considered. The impact of the constraints that prevent the interconnection of substations in the restoration problem is analyzed through the evaluation of the quality of the obtained solutions in comparison with the results of the previous section. Table II presents the results for Case II.

6) Case II – Fault at node 3: The number of loops that can be formed is set to its maximum. The obtained result is the same as that of the radial solution described in subsection III-A1 and Table I.

7) Case II – Fault at node 14: The solution considering radial operation has been detailed in subsection III-A2 and Table I. By allowing the formation of one loop, the obtained solution is the same as the result presented in subsection III-A2 (with one loop). By increasing the number of loops allowed to be formed in the system, no additional improvement is achieved.

TABLE III

RESULTS FOR THE 53-NODE SYSTEM WITH DGS IN CONNECTED OPERATION – CASE III

Faulted node	# of loops	Switching operations	Switches opened	Switches closed	Disconnected nodes	Active load curtailment (kW)	Active load restored (%)	Time (s)
3	0	6	7-4, 26-27, 34-33	8-33, 35-40, 28-50	26	831.60	88.79	4.53
	3	1	7-4	8-25, 8-33, 35-40, 10-38, 28-50	–	0.00	100.00	7.09
14	0	5	16-40, 42-41, 46-47	35-40, 28-50	15, 16, 41, 46	4158.00	48.72	3.83
	1	5	16-40, 46-47	28-27, 35-40, 28-50	15, 16, 46	3534.30	56.41	4.19
11, 14	0	15	31-37 22-9, 44-45, 38-44, 33-39, 16-40, 42-41, 46-47	10-31, 13-12, 104-22, 8-33, 35-40, 10-38, 28-50	15, 16, 41, 44, 46	5128.20	70.16	6.42
	4	14	45-12, 21-18, 44-45, 16-40, 46-47	13-12, 18-17, 104-22, 8-25, 28-27, 8-33, 35-40, 10-38, 28-50	15, 16, 45, 46	4088.70	76.21	7.45
11, 14, 21	0	14	45-12, 22-9, 32-39, 33-39, 16-40, 42-41, 46-47	13-12, 18-17, 104-22, 8-33, 35-40, 10-38, 28-50	15, 16, 32, 41, 46	5336.10	72.70	6.08
	4	13	45-12, 44-45, 16-40, 46-47	13-12, 18-17, 104-22, 8-25, 28-27, 8-33, 35-40, 10-38, 28-50	15, 16, 45, 46	4088.70	79.08	5.55

TABLE IV

RESULTS FOR THE 53-NODE SYSTEM THAT AVOID THE INTERCONNECTION OF SUBSTATIONS WITH DGS IN CONNECTED OPERATION – CASE IV

Faulted node	# of loops	Switching operations	Switches opened	Switches closed	Disconnected nodes	Active load curtailment (kW)	Active load restored (%)	Time (s)
3	3	7	6-5, 28-6	28-27, 8-33, 40-41, 35-40, 28-50	6	485.10	93.46	11.02
14	1	5	16-40, 46-47	28-27, 35-40, 28-50	15, 16, 46	3534.30	56.41	7.64
11, 14	1	16	31-37, 22-9, 44-45, 32-39, 36-35, 16-40, 42-41, 46-47	10-31, 13-12, 104-22, 8-33, 40-41, 35-40, 10-38, 28-50	15, 16, 32, 36, 46	4920.30	71.37	11.17
11, 14, 21	1	12	31-37, 22-9, 44-45, 42-41, 46-47	10-31, 13-12, 18-17, 104-22, 8-33, 10-38, 28-50	15, 16, 40, 41, 46	5128.20	73.76	9.13

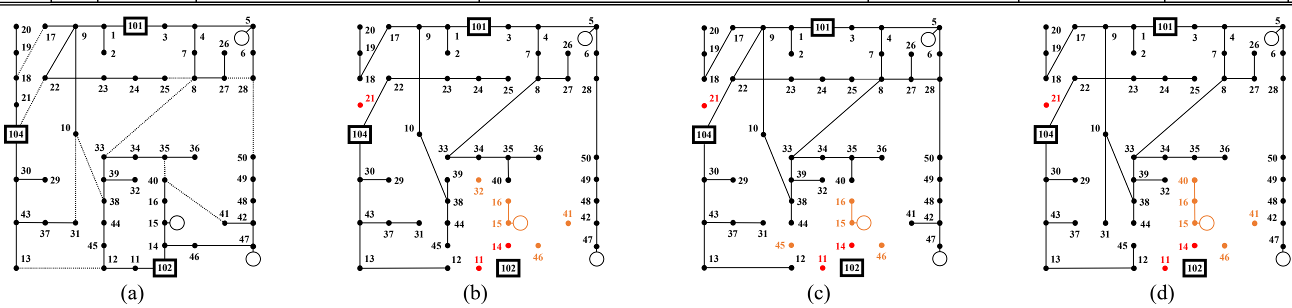

Fig. 4 (a) Prefault configuration of the 53-node system with DGs. Restoration schemes considering simultaneous faults at nodes 11, 14, and 21 with connected operation of the DGs and (b) a radial configuration, (c) four basic loops, and (d) one basic loop without the interconnection of substations.

8) Case II – Faults at nodes 11 and 14: The solution considering a radial topology for this case has been analyzed in subsection III-A3 and Table I. In the next analysis, one loop is allowed in the solution, and the obtained result is shown in Table II. It is important to note that the solution found in this subsection has 6.85% less load restored than the solution found in subsection III-A3, with one operational loop. The amount of load restored decreases as the loop formation is constrained between feeders among the same substation. Finally, by allowing additional loops in the system, the solution to the problem is not improved.

9) Case II – Faults at nodes 11, 14, and 21: The radial solution for this case has been described in subsection III-A4 and Table I. Table II shows the solution when one loop is allowed in the system. The obtained solution has 5.67% less load restored than the result achieved in subsection III-A4, with one operational loop. Again, by allowing additional loops in the system, the solution to the problem is not improved.

10) Case II – Comments on the results when the interconnection of substations is avoided: According to the results of Table I and Table II, the following comments can be made:

- In all the tests performed, the solutions obtained with closed-loop configurations in the restorative state are of equal or better quality than the results achieved with radial configurations.
- In the test cases with multiple faults (at nodes {11, 14} and {11, 14, 21}), different solutions are found when assuming one operational loop in comparison with the results presented in Table I. Also, these solutions have a lower value of restored load since the interconnection of substations is not allowed.

The initial configuration of the 53-node test system is presented in Fig. 3 (a), in which the dotted lines represent the lines with an open switch in the prefault configuration. Figs. 3 (b)–(e) illustrate the topologies of the system obtained considering a fault at nodes {11, 14, 21} (presented in Table I and Table II), in which the red nodes represent the nodes directly affected by the faults and the orange sections are the portions of the network that cannot be restored. Fig. 3 (b) shows the radial restoration topology. Fig. 3 (c) shows the configuration with one loop, in which the substations at nodes 101 and 104 are interconnected. In the configuration presented in Fig. 3 (d), two loops were formed, one among the feeders of the substation at node 101, and the other interconnecting the substations at nodes 101 and 104. Finally, Fig. 3 (e) shows a configuration in which one loop is formed, but the interconnection of substations is not allowed.

TABLE V
RESULTS FOR THE 53-NODE SYSTEM WITH DGS IN ISLANDED OPERATION – CASE V

Faulted node	# of loops	Switching operations	Switches opened	Switches closed	Disconnected nodes	Active load curtailment (kW)	Active load restored (%)	Time (s)
3	0	6	7-4, 26-27, 34-33	8-33, 35-40, 28-50	26	831.60	88.79	5.53
	3	1	7-4	8-25, 8-33, 35-40, 10-38, 28-50	–	0.00	100.00	5.00
14	0	6	16-15, 16-40, 42-41, 46-47	35-40, 28-50	16, 41, 46	3187.80	60.68	3.88
	1	6	16-15, 16-40, 46-47	28-27, 35-40, 28-50	16, 46	2564.10	68.38	4.03
11, 14	0	16	31-37, 16-15, 22-9, 44-45, 38-44, 33-39, 16-40, 42-41, 46-47	10-31, 13-12, 104-22, 8-33, 35-40, 10-38, 28-50	16, 41, 44, 46	4158.00	75.81	10.17
	4	15	45-12, 16-15, 21-18, 44-45, 16-40, 46-47	13-12, 18-17, 104-22, 8-25, 28-27, 8-33, 35-40, 10-38, 28-50	16, 45, 46	3118.50	81.85	5.83
11, 14, 21	0	15	45-12, 16-15, 22-9, 32-39, 33-39, 16-40, 42-41, 46-47	13-12, 18-17, 104-22, 8-33, 35-40, 10-38, 28-50	16, 32, 41, 46	4365.90	77.66	6.28
	4	14	45-12, 16-15, 44-45, 16-40, 46-47	13-12, 18-17, 104-22, 8-25, 28-27, 8-33, 35-40, 10-38, 28-50	16, 45, 46	3118.50	84.04	4.28

TABLE VI
RESULTS FOR THE 53-NODE SYSTEM THAT AVOID THE INTERCONNECTION OF SUBSTATIONS WITH DGS IN ISLANDED OPERATION – CASE VI

Faulted node	# of loops	Switching operations	Switches opened	Switches closed	Disconnected nodes	Active load curtailment (kW)	Active load restored (%)	Time (s)
3	3	7	6-5, 28-6	28-27, 8-33, 40-41, 35-40, 28-50	6	485.10	93.46	13.11
14	1	6	16-15, 16-40, 46-47	28-27, 35-40, 28-50	16, 46	2564.10	68.38	8.48
11, 14	1	17	31-37, 16-15, 22-9, 44-45, 32-39, 36-35, 16-40, 42-41, 46-47	10-31, 13-12, 104-22, 8-33, 40-41, 35-40, 10-38, 28-50	16, 32, 36, 46	3950.10	77.02	16.23
11, 14, 21	1	13	31-37, 16-15, 22-9, 44-45, 42-41, 46-47	10-31, 13-12, 18-17, 104-22, 8-33, 10-38, 28-50	16, 40, 41, 46	4158.00	78.72	8.64

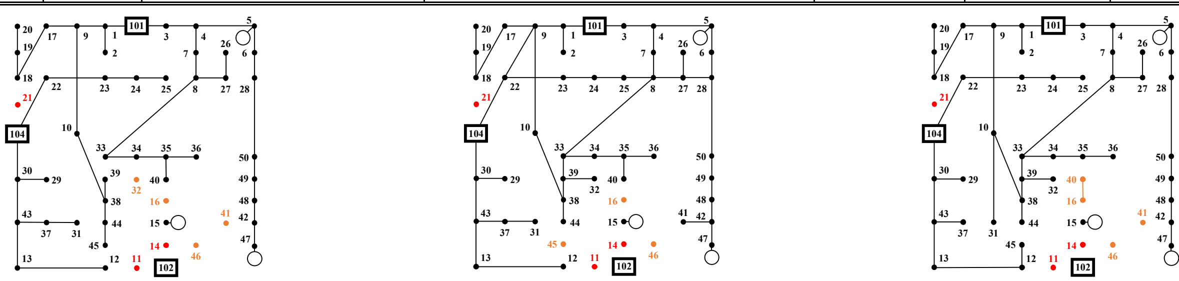

(a) (b) (c)

Fig. 5 Restoration schemes for the 53-node system with DGs considering simultaneous faults at nodes 11, 14, and 21 with islanded operation of the DGs and (a) a radial configuration, (b) four basic loops, and (c) one basic loop without the interconnection of substations.

The results for Case III, which considers the connected operation of the DGs, are summarized in Table III. For each fault scenario, Table III shows that the DGs improve the amount of active load restored, except for a fault at node 14 with closed-loop operation, in which the amount of load restored is the same as for the topology with four loops presented in Table I. Note, however, that in the solution presented in Table III, the number of basic loops formed is only one, and only five switching operations are performed (for the solution of Table I, four loops are formed in the system, and twelve switching operations are performed).

Table IV presents the results for Case IV, which considers the connected operation of the DGs and the interconnection of substations is not allowed. It is also possible to verify that, for all cases, the amount of active restored is higher when compared to the corresponding solutions of Case II, when DGs are not considered in the restoration process.

Fig. 4 shows the restoration topologies for the 53-node system considering the connected operation of the DGs for considering faults at nodes 11, 14, and 21. Note that, in Fig. 4 (b)–(d), the DG at node 15 is not operating since the system does not have enough capacity to reconnect nodes 15 and 16 (Fig. 4 (b) and (c)) and nodes 15, 16, and 40 (Fig. 4 (d)).

The results for Case V and Case VI, presented in Table V and Table VI, respectively, show that by allowing the islanded operation of the DGs, except for the fault at node 3, the amount of active load restored is higher when compared to the fault scenarios of Cases III and IV, as expected, since the operation of the system has more flexibility. Fig. 5 shows that for simultaneous faults at nodes 11, 14, and 21, the DG at node 15 operates in islanded mode, supplying only the demand of its node.

By performing a sensitivity analysis for the solutions obtained for the 53-node system, it is possible to verify the influence of the costs present in the objective function on the percentage of active load restored. First, it is considered a fixed value for $\sigma_i = 10.00$ US\$/kW for all demand nodes, and initial values for $\tau_{ij} = \eta_{ij} = 1.00$ US\$ for all branches, $\gamma = 10.00$ US\$, $\lambda_i^P = 0.01$ US\$/kW, and $\lambda_i^Q = 0.01$ US\$/kVAr for all DGs. These were the values used in the tests. Then, by varying τ_{ij} and η_{ij} simultaneously from US\$ 0.00 up to US\$ 30,000.00, it can be verified that the percentages of active load restored are reduced from the values presented in Table I – Table VI until 0.00%. Additionally, when closed-loop operation is allowed, by increasing γ from US\$ 0.00 up to US\$ 10,000.00, the percentages of active load restored are also reduced from their values for

TABLE VII
RESULTS FOR THE 2313-NODE SYSTEM

Faulted section	# of loops	Switching operations	Switches opened	Switches closed	Active load curtailment (kW)	Active load restored (%)	Time (s)
8, 11, 10, 68	0	1	–	1303-396	2173.36	52.96	8.06
66, 23, 67, 20	0	6	332-232, 307-332, 1242-2297	1301-1279, 940-2297, 1299-586	5397.10	39.37	184.66
	2	9	71-43, 180-132, 247-332	505-2297, 940-2297, 1308-644, 1299-586, 1303-396, 655-572	3932.70	55.82	100.69
26, 50	0	10	375-474, 478-1680, 480-410, 408-432, 951-949, 175-139, 969-1045	393-1046, 149-146, 1303-396	9082.72	9.45	92.33
	3	15	307-332, 374-501, 436-404, 375-474, 478-1680, 480-410, 484-376, 1201-2289, 484-992	1301-1279, 940-2297, 1079-1136, 1299-586, 1303-396, 186-71	8184.11	18.41	345.19
6	0	5	697-676, 646-602	646-816, 1308-644, 799-800	682.43	83.61	67.44
	1	3	–	646-816, 799-800, 655-572	0.00	100.00	13.86
7	0	4	804-710, 815-816	646-816, 799-800	355.25	94.88	78.81
	1	2	–	646-816, 799-800	0.00	100.00	12.22

TABLE VIII
RESULTS FOR THE 2313-NODE SYSTEM THAT AVOID THE INTERCONNECTION OF SUBSTATIONS

Faulted section	# of loops	Switching operations	Switches opened	Switches closed	Active load curtailment (kW)	Active load restored (%)	Time (s)
8, 11, 10, 68	0	1	–	1303-396	2173.36	52.96	31.86
66, 23, 67, 20	2	13	804-674, 1201-2289, 594-619, 646-602, 815-816	1301-1279, 658-802, 940-2297, 799-800, 1299-586, 655-572, 725-606, 1307-615	3932.70	55.82	532.92
26, 50	1	9	480-410, 408-432, 951-949, 175-139, 969-1045	393-1046, 149-146, 1303-396, 186-71	8951.76	10.76	272.00
6	0	5	697-676, 646-602	646-816, 1308-644, 799-800	682.43	83.61	73.98
7	1	8	594-619, 815-816, 332-1296	658-802, 505-2297, 646-816, 799-800, 655-572	0.00	100.00	215.33

closed-loop operation until the values obtained for radial solutions, i.e., no loop is formed in the system. Finally, by increasing simultaneously λ_i^P from 0.00 US$/kW and λ_i^Q from 0.00 US$/kVAr up to 10.00 US$/kW and 10.00 US$/kVAr, respectively, less load is restored, since the redispatch of the DGs is penalized.

The computational times to solve the problem considering both connected and islanded operation of the DGs are between 3.83 s and 16.23 s, which are adequate for the problem.

B. Results for the 2313-node system

To evaluate the scalability of the proposed formulation to solve the restoration problem in a large system, five single and multiple fault scenarios are considered in the 2313-node system. The DGs can only operate connected to the main system. Table VII shows that, except for a simultaneous fault at sections 8, 11, 10, and 68, the temporary closed-loop operation provides solutions with higher amounts of active load restored when compared to the radial topologies when the interconnection of different substations is allowed.

Table VIII also shows that by considering temporary closed-loop operation and not allowing the interconnection of substations it is possible to obtain solutions with more load restored when compared to the radial topologies, except for a simultaneous fault at sections 8, 11, 10, and 68, and a single fault at section 6.

The computational times to solve the restoration problem considering the 2313-node system are between 8.06 s and 532.92 s, which are also adequate for the problem. It should be noted that faster solution times can be achieved by using more powerful computer systems.

The feasibility of all the results was verified using an exact power flow algorithm. This analysis indicated that the operational constraints of both networks are fulfilled in all the cases, what demonstrates the precision of the formulation.

IV. CONCLUSION

This work presented a new mixed-integer second-order cone programming model to solve the service restoration problem in distribution systems, considering a temporary closed-loop topology operation during the restorative state and both connected and islanded operation of distributed generators (DGs). The proposed model is flexible since it allows or not the interconnection of substations in the solution. Also, the maximum number of basic loops in the system can be predefined, or the model can find the minimum number of basic loops that allows more load to be reconnected.

The results show that the formation of temporary operational loops improves the quality of the solutions of the problem since the amount of load curtailment is reduced in comparison with solutions obtained assuming only radial topologies. Moreover, the redispatch of the DGs improved restoration plans, especially when the islanded operation was considered. It should be noted that the proposed strategy does not require the installation of any new equipment in the system. Thus, distribution companies could avoid future economical investments for improving reliability indexes by applying the proposed strategy.

The proposed model can be extended to consider other aspects of the restoration problem, including unbalanced network operation. Besides that, other devices present in distribution systems, such as voltage control equipment and energy storage systems, can also be modeled to improve the restoration process.

References

[1] S. Ćurčić, C. S. Özveren, L. Crowe, and P. K. L. Lo, "Electric power distribution network restoration: a survey of papers and a review of the restoration problem," *Electr. Power Syst. Res.*, vol. 35, no. 2, pp. 73–86, Nov. 1995.

[2] A. Zidan *et al.*, "Fault detection, isolation, and service restoration in distribution systems: state-of-the-art and future trends," *IEEE Trans. Smart Grid*, vol. 8, no. 5, pp. 2170–2185, Sep. 2017.

[3] N. Jenkins, R. Allan, P. Crossley, D. Kirschen, and G. Strbac, *Embedded generation*, 1st ed. Stevenage: IET, 2000.

[4] Y. Li, J. Xiao, C. Chen, Y. Tan, and Y. Cao, "Service restoration model with mixed-integer second-order cone programming for distribution network with distributed generations," *IEEE Trans. Smart Grid*, vol. 10, no. 4, pp. 4138–4150, Jul. 2019.

[5] L. H. Macedo, G. Muñoz-Delgado, J. Contreras, and R. Romero, "Optimal restoration of distribution networks through reconfiguration and microgrid formation," in *2020 IEEE PES Innovative Smart Grid Technologies Europe (ISGT-Europe)*, 2020, pp. 1231–1235.

[6] J. M. Home-Ortiz and J. Roberto Sanches Mantovani, "Resilience enhancing through microgrids formation and distributed generation allocation," in *2020 IEEE PES Innovative Smart Grid Technologies Europe (ISGT-Europe)*, 2020, pp. 995–999.

[7] T. Gönen, *Electric power distribution engineering*, 3rd ed. Boca Raton: CRC Press, 2014.

[8] J. S. Wu, K. L. Tomsovic, and C. S. Chen, "A heuristic search approach to feeder switching operations for overload, faults, unbalanced flow and maintenance," *IEEE Trans. Power Deliv.*, vol. 6, no. 4, pp. 1579–1585, Oct. 1991.

[9] D. Ritter, J. F. Franco, and R. Romero, "Analysis of the radial operation of distribution systems considering operation with minimal losses," *Int. J. Electr. Power Energy Syst.*, vol. 67, pp. 453–461, May 2015.

[10] R. A. V. Peralta, J. B. Leite, and J. R. S. Mantovani, "Automatic restoration of large-scale distribution networks with distributed generators, voltage control devices and heating loads," *Electr. Power Syst. Res.*, vol. 176, pp. 1–11, Nov. 2019.

[11] C.-H. Lee and C.-M. Huang, "Analysis of load transfer on radial distribution systems with tie lines," *Eur. Trans. Electr. Power*, vol. 17, no. 3, pp. 268–284, May 2007.

[12] T. H. Chen, W. T. Huang, J. C. Gu, G. C. Pu, Y. F. Hsu, and T. Y. Guo, "Feasibility study of upgrading primary feeders from radial and open-loop to normally closed-loop arrangement," *IEEE Trans. Power Syst.*, vol. 19, no. 3, pp. 1308–1316, Aug. 2004.

[13] D. Shirmohammadi, "Service restoration in distribution networks via network reconfiguration," *IEEE Trans. Power Deliv.*, vol. 7, no. 2, pp. 952–958, Apr. 1992.

[14] R. M. Ciric and D. S. Popovic, "Multi-objective distribution network restoration using heuristic approach and mix integer programming method," *Int. J. Electr. Power Energy Syst.*, vol. 22, no. 7, pp. 497–505, Oct. 2000.

[15] S. Dimitrijevic and N. Rajakovic, "Service restoration of distribution networks considering switching operation costs and actual status of the switching equipment," *IEEE Trans. Smart Grid*, vol. 6, no. 3, pp. 1227–1232, May 2015.

[16] F. Wang *et al.*, "A multi-stage restoration method for medium-voltage distribution system with DGs," *IEEE Trans. Smart Grid*, vol. 8, no. 6, pp. 2627–2636, Nov. 2017.

[17] S. Riahinia, A. Abbaspour, M. Moeini-Aghtaie, and S. Khalili, "Load service restoration in active distribution network based on stochastic approach," *IET Gener. Transm. Distrib.*, vol. 12, no. 12, pp. 3028–3036, Jul. 2018.

[18] A. A. Hafez, W. A. Omran, and Y. G. Hegazy, "A decentralized technique for autonomous service restoration in active radial distribution networks," *IEEE Trans. Smart Grid*, vol. 9, no. 3, pp. 1911–1919, May 2018.

[19] A. Sharma, D. Srinivasan, and A. Trivedi, "A decentralized multi-agent approach for service restoration in uncertain environment," *IEEE Trans. Smart Grid*, vol. 9, no. 4, pp. 3394–3405, Jul. 2018.

[20] Y. Kumar, B. Das, and J. Sharma, "Multiobjective, multiconstraint service restoration of electric power distribution system with priority customers," *IEEE Trans. Power Deliv.*, vol. 23, no. 1, pp. 261–270, Jan. 2008.

[21] D. S. Sanches, J. B. A. London, and A. C. B. Delbem, "Multi-objective evolutionary algorithm for single and multiple fault service restoration in large-scale distribution systems," *Electr. Power Syst. Res.*, vol. 110, pp. 144–153, May 2014.

[22] S. Wang and H.-D. Chiang, "Multi-objective service restoration of distribution systems using user-centered methodology," *Int. J. Electr. Power Energy Syst.*, vol. 80, pp. 140–149, Sep. 2016.

[23] L. T. Marques, A. C. B. Delbem, and J. B. London, "Service restoration with prioritization of customers and switches and determination of switching sequence," *IEEE Trans. Smart Grid*, vol. 9, no. 3, pp. 2359–2370, May 2018.

[24] R. Romero, J. F. Franco, F. B. Leão, M. J. Rider, and E. S. de Souza, "A new mathematical model for the restoration problem in balanced radial distribution systems," *IEEE Trans. Power Syst.*, vol. 31, no. 2, pp. 1259–1268, Mar. 2016.

[25] H. Sekhavatmanesh and R. Cherkaoui, "Analytical approach for active distribution network restoration including optimal voltage regulation," *IEEE Trans. Power Syst.*, vol. 34, no. 3, pp. 1716–1728, May 2019.

[26] B. Chen, C. Chen, J. Wang, and K. L. Butler-Purry, "Sequential service restoration for unbalanced distribution systems and microgrids," *IEEE Trans. Power Syst.*, vol. 33, no. 2, pp. 1507–1520, Mar. 2018.

[27] B. Chen, C. Chen, J. Wang, and K. L. Butler-Purry, "Multi-time step service restoration for advanced distribution systems and microgrids," *IEEE Trans. Smart Grid*, vol. 9, no. 6, pp. 6793–6805, Nov. 2018.

[28] G. W. Stagg and A. H. El-Abiad, *Computer methods in power system analysis*, 1st ed. New York: McGraw-Hill, 1968.

[29] J. F. Franco, M. J. Rider, and R. Romero, "A mixed-integer quadratically-constrained programming model for the distribution system expansion planning," *Int. J. Electr. Power Energy Syst.*, vol. 62, pp. 265–272, Nov. 2014.

[30] M. S. Lobo, L. Vandenberghe, S. Boyd, and H. Lebret, "Applications of second-order cone programming," *Linear Algebra Appl.*, vol. 284, no. 1–3, pp. 193–228, Nov. 1998.

[31] M. Lavorato, J. F. Franco, M. J. Rider, and R. Romero, "Imposing radiality constraints in distribution system optimization problems," *IEEE Trans. Power Syst.*, vol. 27, no. 1, pp. 172–180, Feb. 2012.

[32] "LaPSEE power system test cases repository," 2021. [Online]. Available: http://www.feis.unesp.br/#!/lapsee. [Accessed: 01-Feb-2021].

[33] R. Fourer, D. M. Gay, and B. W. Kernighan, *AMPL: a modeling language for mathematical programming*, 2nd ed. Duxbury, MA, USA: Thomson, 2003.

[34] IBM, "IBM ILOG CPLEX optimization studio v12.10.0 documentation," 2020. [Online]. Available: https://www.ibm.com/support/knowledgecenter/en/SSSA5P_12.10.0/COS_KC_home.html. [Accessed: 14-Sep-2020].

Renzo Vargas (S'15–M'20) received the B.Sc. degree in electrical engineering from the National University Engineering, Lima, Peru, in 2012, and the M.Sc. and Ph.D. degrees in electrical engineering from the São Paulo State University (UNESP), Ilha Solteira, Brazil, in 2015 and 2019, respectively. Currently, he is carrying out postdoctoral research with the UNESP.

His research interests include the development of methodologies for the optimization and planning of electrical power systems.

Leonardo H. Macedo (S'14–M'18) received the B.Sc., M.Sc., and Ph.D. degrees from the São Paulo State University, São Paulo, Brazil, in 2012, 2015, and 2019, respectively, where he is currently a postdoctoral researcher.

His current research interests include the development of methods for the optimization, planning, and control of electrical power systems.

Juan M. Home-Ortiz received the B.Sc. and M.Sc. degrees in electrical engineering from the Universidad Tecnológica de Pereira, Colombia, in 2011 and 2014, respectively, and the Ph.D. degree in electrical engineering from the São Paulo State University (UNESP), Ilha Solteira, Brazil, in 2019. Currently, he is carrying out postdoctoral research with the UNESP.

His research interests include the development of methodologies for the optimization, planning, and control, of electrical power systems.

Rubén Romero (M'93–SM'08) received the B.Sc. and P.E. degrees from the National University of Engineering, Lima, Peru, in 1978 and 1984, respectively. He received the M.Sc. and Ph.D. degrees from the University of Campinas, Campinas, Brazil, in 1990 and 1993, respectively. He is currently a professor of electrical engineering at the São Paulo State University, Ilha Solteira, Brazil.

His research interests include methods for the optimization, planning, and control of electrical power systems, applications of artificial intelligence in power systems, and operations research.